Nonlinear Dynamics of a Bi-stable Composite Shell for Morphing Applications

A. F. Arrieta, D.J. Wagg and S.A. Neild

Department of Mechanical Engineering,University of Bristol,

University Walk, Bristol, U.K BS8 1TR

Abstract

A reduced order model for the transverse displacement dynamics of a bi-stable composite shell is derived to be used in morphing structures applications. Love's equations of motion for general shells are used with the Von-Karman strain-displacement relations to obtain the governing dynamic equations. A Galerkin approach is employed to obtain a set of modal nonlinear equations describing the solution for the transverse displacement. Frequency and time response diagrams are experimentally obtained and employed to reduce the order of the derived model. The reduced set of nonlinear modal equations are numerically solved to obtained the simulated frequency and time response for the shell. Experimental results are compared to those numerically simulated showing very good agreement. The capability to capture the dynamics of the bi-stable shell with a simple model facilitates its integration with smart actuators rendering feasible the design of morphing structures.

Keywords: Multi-stable composites, nonlinear vibration, morphing structures, subharmonic resonance.

1 INTRODUCTION

Composite laminates are becoming increasingly important in a wide variety of applications, particularly in aerospace engineering. A novel type of composite laminates exhibiting multiple stable configurations, or states, have been the focus of recent research within the adaptive structures community [1]. The property of multi-stability appears as a result of asymmetric residual thermal stresses induced during the curing process [2]. The change between stable configurations is achieved by a strongly nonlinear mechanism known as snap-through. Recent research has focus on the applicability of multi-stable composite laminates to aerospace morphing structures as the tailoring of predetermined stable-shapes has become feasible [3]. By coupling the tailoring of multi-stable composites with smart actuators and control systems morphing structures can be obtained. The operating conditions for morphing applications will inevitably result

in exposure of the multi-stable composites to high levels of dynamic excitation, for example in an aeroelastic environment. Potentially these large amplitude vibrations could lead to unexpected failure of the multi-stable structures or trigger undesired change of shapes (snap-through) [4], therefore vibration suppression mechanisms are required for a robust operation. Successful implementation of such control strategies rely on accurate models describing the dynamics of the structures. However, most of the studies of composite laminates for morphing have focused on models to predict the change of shape of the laminates under static loading [5]. Furthermore, very little work has been carried out to examine the dynamics of multi-stable composite plates. A first attempt to characterize the snap-through was presented in [6] and a study of the dynamic response around stable states was introduced in [7]. However, to the best knowledge of the authors no theoretical models for the dynamics of multi-stable composite laminates intended vibration suppression control has not been attempted on.

This paper presents the development of a dynamic model using Love-Von-Karman theory for shallow shells vibration to obtain the nonlinear governing equations for the transverse displacement of a bi-stable composite shell. A Galerkin solution methodology is employed to decouple the solution of the transverse displacement of the bi-stable shell into time and spatial solutions. A set of nonlinear ordinary differential equations is obtained for the time solution of the transverse displacement. The spatial solution is modelled using beam functions as mode shapes. The model is validated with an experimental characterization based on experimental frequency response diagrams that capture the main dynamic features of the bi-stable plate, such as primary resonance and damping coefficients. This allow us to choose the minimum number of degrees-of-freedom required to obtain a good approximative solution. Secondary subharmonic resonance observed in nonlinear vibration of flat composite plates [8] were also included in the experimental characterization. Previous studies have reported that they can lead to catastrophic failure of structures even if the excitation is away from the natural frequencies of the system as reported in [9]. Simulations for both the frequency and time response are conducted showing excellent qualitative and quantitative match. Furthermore, beam functions approximate qualitatively well the experimentally obtained mode shapes. Finally conclusions are drawn and an outline of future work is presented, including the coupling of the derived dynamic model with smart actuators, such as MFCs, to obtain a truly morphing structure.

2 PROBLEM FORMULATION

The two stable states of the bi-stable shell are shown in figure 1.(a),(b). The shell is mounted to a ling shaker which is used as the source of external excitation. The four edges of the shell can oscillate freely.

2.1 Equations of motion

The equations of motion for the vibrations for a bi-stable composite shell around one of its stable states are obtain from Love-Von-Karman theory for large deflections of shells [10]. We neglected in-plane inertias in our derivation as their effect is of higher order. Using the constitutive laws for a laminated orthotropic material [11] and introducing Airy's stress function $\phi(x, y, t)$, the equation for the transverse displacement is

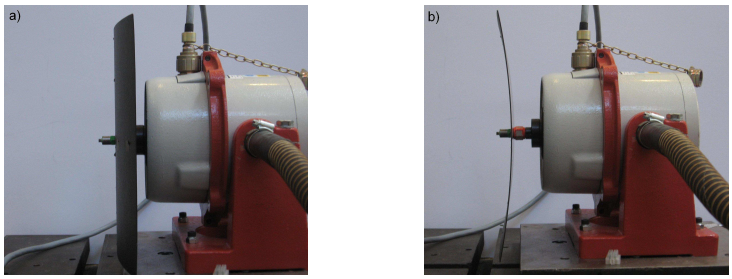

(a) Stable state 1 (b) Stable state 2

Figure 1: Stable configurations of the Bi-stable plate.

given by

$$D_{11}\frac{\partial^4 w}{\partial x^4} + 2(D_{12}+D_{33})\frac{\partial^4 w}{\partial x^2 \partial y 2} + D_{22}\frac{\partial^4 w}{\partial y^4} + \frac{1}{R_x}\frac{\partial^2 \phi}{\partial y^2} + \frac{1}{R_y}\frac{\partial^2 \phi}{\partial x^2} \tag{1}$$
$$+\frac{\partial^2 \phi}{\partial y^2}\frac{\partial^2 w}{\partial x^2} + \frac{\partial^2 \phi}{\partial x^2}\frac{\partial^2 w}{\partial y^2} - 2\frac{\partial^2 w}{\partial x \partial y}\frac{\partial^2 \phi}{\partial x \partial y} + C\dot{w} + \rho h\ddot{w} = q_3(x,y,t).$$

coupled to a compatibility equation

$$P_{11}\frac{\partial^4 \phi}{\partial y^4} + P_{22}\frac{\partial^4 \phi}{\partial x^4} + (P_{33} - 2P_{12})\frac{\partial^4 \phi}{\partial x^2 \partial y^2} = \frac{1}{R_x}\frac{\partial^2 w}{\partial y^2} + \frac{1}{R_y}\frac{\partial^2 w}{\partial x^2} + (\frac{\partial^2 w}{\partial x \partial y})^2 - \frac{\partial^2 w}{\partial x^2}\frac{\partial^2 w}{\partial y^2}, \tag{2}$$

where R_i is the radius of curvature of the $_i$ coordinate, P_{ij} are given by $(P_{11}, P_{12}, P_{22}) = \frac{(A_{22}, A_{12}, A_{11})}{A_{11}A_{22} - A_{12}^2}$ and $P_{33} = \frac{1}{A_{66}}$, A_{ij} and D_{ij} are the membrane and bending stiffness relating direction i with j, C is the matrix of viscous damping coefficients, h is the thickness and ρ the density of the plate. Airy's stress function is defined as [12]

$$N_x = \frac{\partial^2 \phi}{\partial y^2}, N_y = \frac{\partial^2 \phi}{\partial x^2}, N_{xy} = -\frac{\partial^2 \phi}{\partial x \partial y}, \tag{3}$$

where N_{ij} are the membrane forces. The nonlinear equations 1 and 2 govern the transverse displacement of the bi-stable composite about its stable states.

We assume a separable solution for the transverse displacement in equation 1 given by $w(x,y,t) = X(x)Y(y)W(t)$. Further, the spatial functions $X(x)$ and $Y(y)$ or mode shapes are assumed to have the form of beam functions [13]

$$X(x) = F_{x1}\sin(E_{x1}x) + F_{x2}\cos(E_{x2}x) + F_{x3}\sinh(E_{x3}x) + F_{x4}\cosh(E_{x4}x) \tag{4}$$
$$Y(y) = F_{y1}\sin(E_{y1}y) + F_{y2}\cos(E_{y2}y) + F_{y3}\sinh(E_{y4}y) + F_{y4}\cosh(E_{y4}y). \tag{5}$$

In our study we consider a bi-stable shell with free-edge boundary conditions, namely

$$\begin{aligned} N_x(0,y) = N_x(L_x,y) = N_y(x,0) = N_y(x,L_y) = 0 \\ N_{xy}(0,y) = N_{xy}(L_x,y) = N_{xy}(x,0) = N_{xy}(x,L_y) = 0 \\ M_x(0,y) = M_x(L_x,y) = M_y(x,0) = M_y(x,L_y) = 0 \\ Q_x(0,y) = Q_x(L_x,y) = Q_y(x,0) = Q_y(x,L_y) = 0, \end{aligned} \tag{6}$$

where L_x=L_y are the dimensions of the bi-stable shell. The expression for the mode shapes are obtained substituting the selected beam functions 4 in the stated boundary conditions.

2.2 Galerkin method solution

A Galerkin solution approach is followed in order to obtain a solution for the transverse displacement from equations 1 and 2 [14]. As the equations are coupled we first need to find a solution for the stress function ϕ to obtain the tranverse displacement w. To this end, we notice that in equation 2, w and ϕ are decoupled. Therefore we can treat it as a linear partial differential equation of ϕ forced by an arbitrary function of w.

$$P_{11}\frac{\partial^4\phi}{\partial y^4} + P_{22}\frac{\partial^4\phi}{\partial x^4} + (P_{33} - 2P_{12})\frac{\partial^4\phi}{\partial x^2\partial y^2} = h(X(x), Y(y), W(t)). \tag{7}$$

Recalling that equation 7 is linear in ϕ, a particular solution will be of the same form as the forcing function h, this is $\phi(x, y, t) = h^*(w)$, where individual terms in h^* and h are related by proportional constants. The particular solution $h^*(w)$ for ϕ enable us to solve the transverse displacement equation. Following the Galerkin procedure we rewriting the solution for w as $w(x, y, t) = \sum_{n=1}^{\infty} X_n(x)Y_n(y)W_n(t)$ and substitute it with function $h^*(w)$ into equation 1 to obtain a set of modal equations given by

$$\sum_{n=1}^{\infty} X_n(x)Y_n(y)[\rho h\ddot{W}_n + 2\zeta_n\dot{W}_n] + \sum_{n=1}^{\infty}\eta_{n1}W_n(t) + \sum_{n=1}^{\infty}\eta_{n2}W_n(t)^2 + \sum_{n=1}^{\infty}\eta_{n3}W_n(t)^3 = q_3(x, y, t), \tag{8}$$

where η_{ni} are coefficients function of $X(x)$, $Y(y)$ and $h^*(w)$. The solutions of the modal equations gives the time response of the transverse displacement w, which will be solved numerically in section 4.1.

3 DYNAMIC RESPONSE AND MODEL REDCUTION

In order to reduced the order of the governing equation 8 we conducted a process of characterization of the dynamic response of the bi-stable shell. This process and its results are presented in the following sections.

3.1 Experimental assembly and measurement procedure

A carbon-fibre epoxy $[0_4 - 90_4]_T$ 300x300 mm square bi-stable laminate was used as the experimental specimen the experimental assembly used for this study can be seen in figure 2.(a). The shell was characterized by measuring the experimental frequency response for 2 points on the coordinate directions of a local frame with the axes (x, y) coinciding with the curved and flat directions of the bi-stable plate as seen in figure 2.(b). The out-of-plane z axis is chosen for the transverse direction.
The frequency response diagrams for the system were obtained by a process of stroboscopic sampling of the time series for the measured displacement data. By exciting the system with a sinusoidal input to induce vibration, peak-to-peak displacement measurements were sampled from the time responses for several consecutive forcing periods, as shown in figure 3. The sampled amplitude value over one forcing period represents a single point in a frequency response diagram. For a given forcing frequency the sampled amplitude for a linear system over consecutive forcing periods remains unchanged, as seen in figure 3.(a). On the other hand, a nonlinear response can exhibit multiple measured amplitudes values over consecutive forcing periods as seen in figure 3.(b).

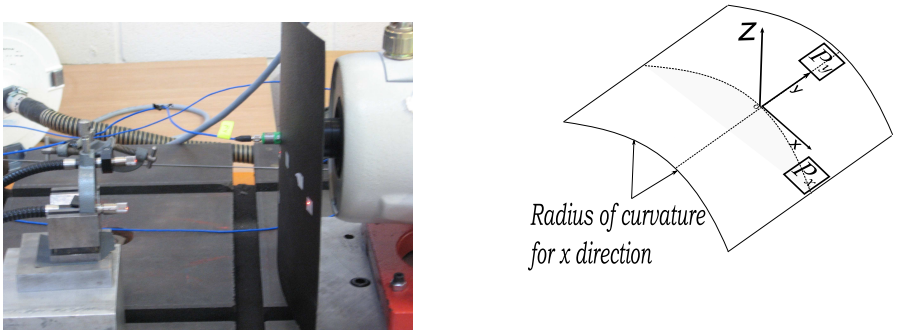

(a) (b)

Figure 2: (a) Experimental Assembly. Ling shaker V405, vibrometer OFV-552. b) Measured points in the laminate. Point P_x describes the transverse vibration in curved-direction, coinciding with the x-coordinate. Point P_y describes the transverse vibration in the flat-direction.

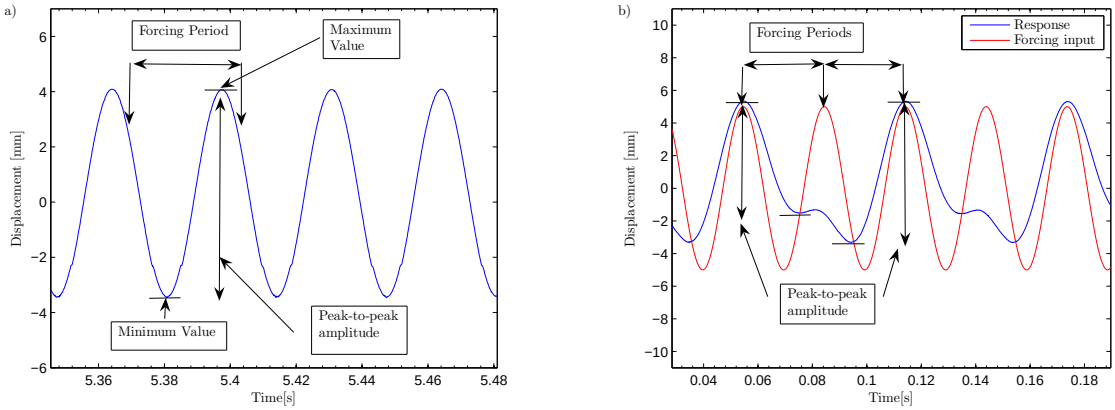

(a) (b)

Figure 3: Stroboscopic sampling procedure to obtain peak-to-peak values for a given forcing period. For a a) linear response and b) nonlinear response.

3.2 Time and frequency response

The experimental frequency response diagram for the curved direction, i.e. for point P_x, of the shell for a forcing amplitude of 1 N is shown in figure 4.(a). Two modes of vibration dominate the response, mode x_1 at 17.6 Hz and mode x_2 at 29.6 Hz. Damping coefficients ζ_{x_1} and ζ_{x_2}, are chosen based on the peaks for the response for each mode. A linear response is seen in most of the studied range except for the region around 35 Hz. This range corresponds with twice the natural frequency for mode x_1. In more detail the nonlinear displacement response for point P_x for a forcing frequency of 34.2 Hz is shown in figure 4.(b). A non sinusoidal response to the simple harmonic excitation of the shell is observed. The power spectrum of this response, figure 4.(c), shows that the energy transmitted by the external forcing at 34.2 Hz is almost completely transferred to a lower frequency at around 17.6 Hz, coinciding with the measured natural frequency of mode x_1. The above mentioned experimental observations suggest that a 1/2 sub-harmonic response of mode x_1 is present in the response [15]. Figure 4.(d) shows the experimental frequency response diagram describing the flat direction of the shell. A

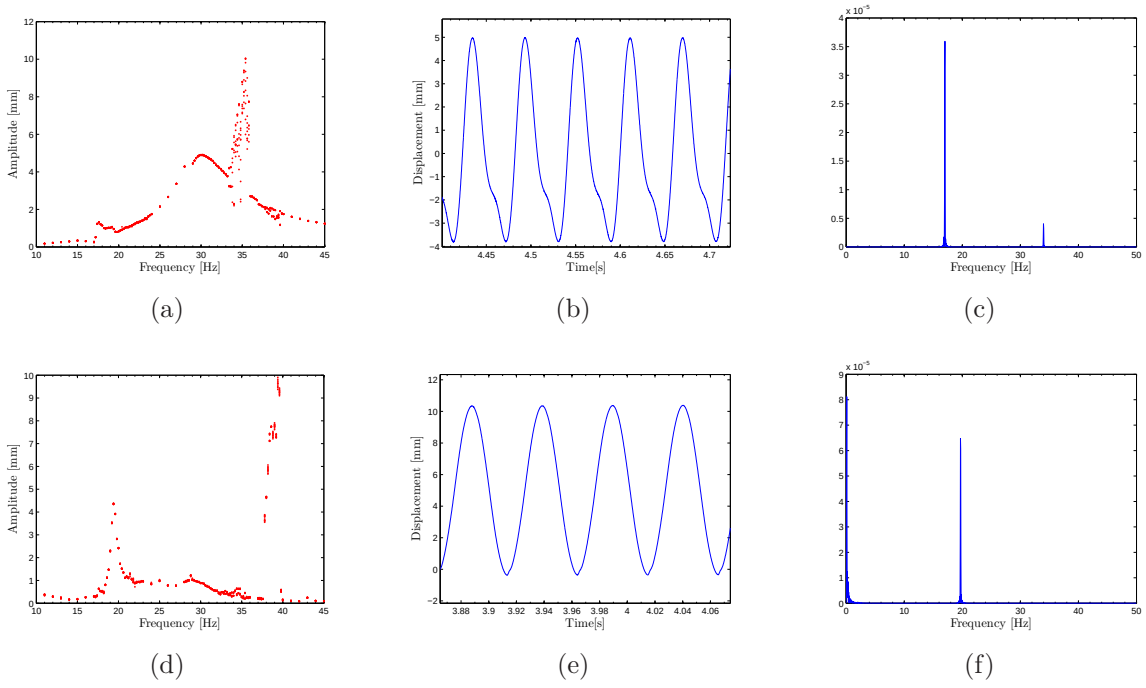

Figure 4: Experimental results, forcing amplitude of $F_o = 1.0\ N$, frequency range Ω=[11, 45] Hz. (a) frequency response for point P_x. b) displacement time response and c) power spectrum for a harmonic input at $\Omega = 34.2$ Hz. (d) frequency response for point P_y. (e) displacement time response and (f) power spectrum for a harmonic input at $\Omega = 39.2$ Hz.

single mode dominates the response, that is mode x_3 at 19.6 Hz. Similarly to mode x_1, ζ_{x_3} is chosen based on the peak for the response of mode x_3. A small response around 30 Hz can be seen suggesting weak coupling between the response of x_3 and x_2. In a similar way as for the curved direction of the shell, nonlinear oscillations were observed on the range of twice the frequency of mode x_3. Figures 4.(e) and 4.(f) show a displacement time series and power spectrum for a forcing frequency opf 39.2 Hz. The displacement response displays a sinusoidal behaviour. However the power spectrum graphs shows once more that most of the energy from the forcing input is transferred from the forcing frequency to a lower frequency at around 19 Hz, matching the frequency of mode x_3. Yet again, the observed experimental characteristics correspond to a 1/2 subharmonic behaviour of mode x_3.

A 1/2 subharmonic resonance was observed for both the flat and curved direction. Well established theoretical results state that quadratic type nonlinearities generate 1/2 subharmonic oscillations [16]. Other super or subharmonic oscillations were sought but not found for different levels of forcing. As a result, we choose to keep only this type of nonlinearity in the modal equations. The reduced set of equations of motion for the bi-stable shell are discussed in the next section.

3.3 Modal equations

The experimental results for the dynamic response of the shell show that it is dominated by 3 modes, enabling us to reduced the number of modal equations in the solution for w. Furthermore, for the current configuration only the quadratic nonlinear terms are

important in the response simplifying the system of modal equations 8 to

$$\ddot{x_1} + 2\zeta_{x_1}\omega_{x_1}\dot{x_1} + \omega_{x_1}^2 x_1 + \alpha_1 x_1^2 + \alpha_2 x_1 x_2 = f_{x_1} F_o \sin\Omega t, \tag{9}$$

$$\ddot{x_2} + 2\zeta_{x_2}\omega_{x_2}\dot{x_2} + \omega_{x_2}^2 x_2 = f_{x_2} F_o \sin\Omega t, \tag{10}$$

$$\ddot{x_3} + 2\zeta_{x_3}\omega_{x_3}\dot{x_3} + \omega_{x_3}^2 y_1 + \beta_1 {x_3}^2 + \beta_2 x_3 x_2 = f_{x_3} F_o \sin\Omega t, \tag{11}$$

where x_i is the transverse displacement for mode x_i, F_o is the driving force amplitude, Ω is the forcing frequency, $f_{x_i}(x, y)$ are the modal participation factor for mode x_i, α_1,α_2,β_1 and β_2 are constant coefficient.

4 SIMULATION RESULTS AND COMPARISON

4.1 Simulated frequency and time response

The coefficients proposed for the derived equations of motion were fitted using the frequency response diagrams obtained experimentally. The set of ordinary coupled non-

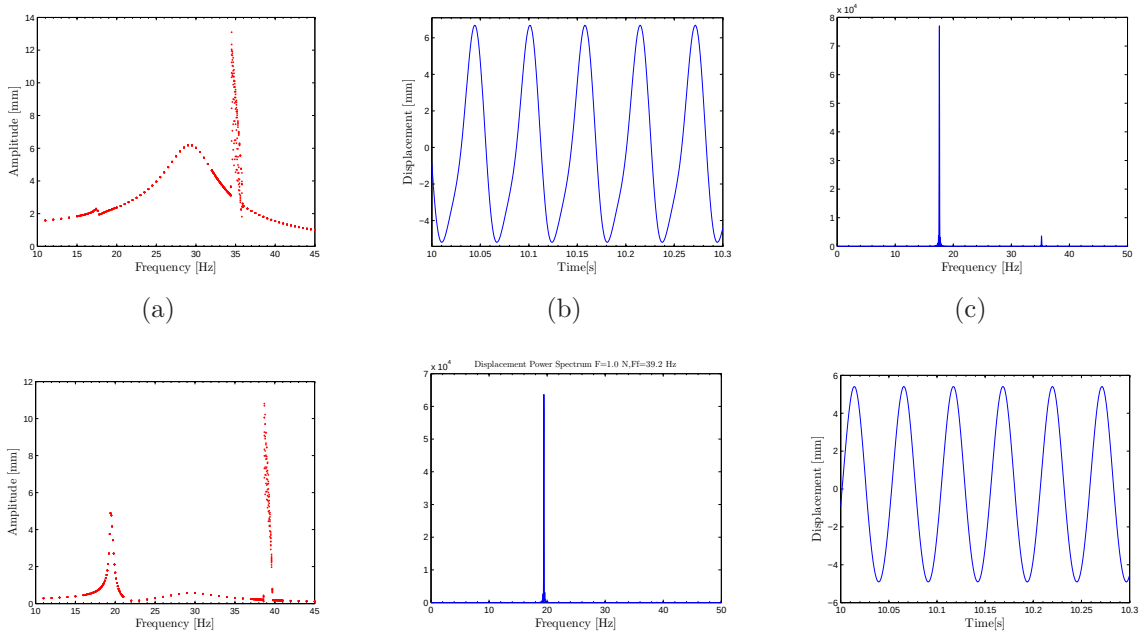

Figure 5: Numerically simulated dynamic response for the curved direction. $F_o = 1.0\ N$, frequency range Ω=[11, 45] Hz (a) frequency response diagram for the curved direction. (b) displacement time response. (c) displacement power spectrum. Forcing frequency = 34.2 Hz. (d) frequency response diagram for the flat direction. (e) displacement time response flat direction. (f) displacement power spectrum flat direction. Forcing frequency = 39.2 Hz.

linear differential equations derived for the identified modes, equations 9, 10 and 11, were solved simultaneously using a Runge-Kutta type solver. Figure 5 show the simulated results obtained for the frequency and time response for the shell. When compared with the experimental results shown in figure 4 very good qualitative and quantitative agreement can be observed in both the frequency response diagrams and displacement and power spectrum graphs. The frequency response diagrams for both the curved and

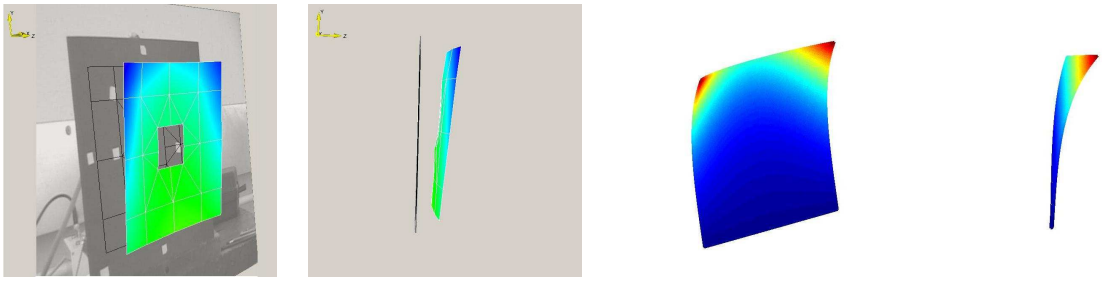

(a) (b) (c) (d)

Figure 6: Experimental and simulated mode shape for mode x_3. (a) Three-dimensional view and (b) lateral view of the experimental transverse displacement. (c) Three-dimensional view and (d) lateral view of the simulated transverse displacement.

flat directions, figures 5.(a) and 5.(d), show all the relevant measured characteristics, including the observed subharmonic oscillations. Similarly, the time response and power spectrum graphs show excellent agreement with the experimental results. In particular, the waveform and energy transfer for the subharmonic oscillations are captured, demonstrating the validity of the model.

4.2 Experimental and simulated mode shapes

The mode shapes of the bi-stable shell were obtained by exciting the shell at the previously identified natural frequencies and measured using a scanning laser. The simulated mode shapes are obtained by only keeping the non-zero coefficients in beam functions 4, this gives for mode x_3

$$X(x) = 0.1 * \cosh(\frac{\pi x}{L_x}), \qquad Y(y) = \sinh(\frac{\pi y}{L_y}) + 0.9 * \cosh(\frac{\pi y}{L_y}), \tag{12}$$

where L_x=L_x=300 mm. To illustrate the results figure 6 shows both the experimental and simulated mode shapes for mode x_3. Comparing the image of the experimental displacement field showed in figures 6.(a) and 6.(b) to the simulated mode shape shown in 6.(c) and 6.(d) it can be seen that a good qualitative agreement was achieve. Thus, the mode shapes for a bi-stable shell can be modelled using beam functions with a good level of accuracy.

5 CONCLUSIONS

The main objective of this paper was to derive a reduced order model to capture the dynamics of a bi-stable composite shell for adaptive structures applications. Love's-Von-Karman theory for shallow shell deflection was used to obtain the equations of motion for the bi-stable shell. A Galerkin approach and an experimental characterization process were employed to reduced the order of the model. A separable solution for the transverse displacement was obtained by numerically solving a set of modal nonlinear equations multiplied by the associated mode shapes functions. A comparison between the experimental and the simulated frequency response diagrams showed that the model reproduces accurately the observed dynamics of the plate. The natural frequencies for the modes in the range of interest were capture. Moreover, the potentially dangerous

subharmonic oscillations were modelled with the nonlinearities included in the equations of motion. Additionally, experimental mode shapes were modelled using mode shapes showing good qualitative agreement.

The simplicity of the derived reduced order model facilitates its integration to relatively low order adaptive controllers and smart actuators to obtain morphing structures. Furthermore, the use of the measured mode shapes with the frequency response diagrams allows for a better selection for the position of smart actuators for vibration cancellation and actuation control of the bi-stable shell. New developments will seek to integrate the derived model with the effect of the smart actuators to achieve the mentioned control objectives.

ACKNOWLEDGEMENTS

The authors would like to acknowledge the support of the ORS scheme; Andres F. Arrieta is funded through an ORS scholarship, and the EPSRC; David Wagg is supported by an Advanced Research Fellowship.

References

[1] M.-L. Dano and M.W. Hyer. Thermally-induced deformation behavior of unsymmetric laminates. *International Journal of Solids and Structures*, 35:2101–2120, 1998.

[2] M.R. Schultz and M.W. Hyer. Snap-through of unsymmetric cross-ply laminates using piezoceramic actuators. *Journal of intelligent material systems and structures*, 14:795–814, 2003.

[3] K D. Potter and P.M. Weaver. A concept for the generation of out-of-plane distortion from tailored frp laminates. *Composites*, 35:1353–1361, 2004.

[4] I.K. Oh, J.H. Han, and I. Lee. Thermopiezoelastic snapping of piezolaminated plates using layerwise nonlinear finite elements. *AIAA Journal*, 39(6):1188–1197, June 2001.

[5] M.-L. Dano and M.W. Hyer. Snap-through of unsymmetric fiber-reinforced composite laminates. *International Journal of Solids and Structures*, 39:175–198, 2002.

[6] A.F. Arrieta, F. Mattioni, S.A. Neild, P.M. Weaver, D.J. Wagg, and K. Potter. Nonlinear dynamics of a bi-stable composite laminate plate with applications to adaptive structures. In *2nd European Conference for Aero-Space Sciences*, 2007.

[7] A. F. Arrieta, , S. Neild, and D. Wagg. Nonlinear dynamic response and modelling of a bi-stable composite plate for applications to adaptive structures. *Submitted to Nonlinear Dynamics*, 2008.

[8] A.H. Nayfeh and D.T. Mook. *Nonlinear Oscillations*. John Wiley & Sons, 1979.

[9] T. Von Karman. The engineer grapples with nonlinear problems. *Bulletin of American Mathematical Society*, 46:615–683, 1940.

[10] P.F Pai and A. H. Nayfeh. A unified nonlinear formulation for plate and shell theories. *Nonlinear Dynamics*, 6:459–500, 1994.

[11] D. Gay, S.V. Hoa, and S. W. Tsai. *Composite Materials: Design and Applications*. CRC Press, 2002.

[12] W. Nowacki. *Dynamics of Elastic Systems*. John Wiley & Sons, 1963.

[13] W. Soedel. *Vibration of shells and plates*. Marcel Dekker, Inc., 2004.

[14] A.W. Leissa and A.S. Kadi. Curvature effects on shallow shell vibrations. *Journal of Sound and Vibration*, 16 (2):173–187, 1971.

[15] A.H. Nayfeh. *Nonlinear Interactions*. John Wiley & Sons, 2000.

[16] B. Balachandran and A. H. Nayfeh. Observations of modal interactions in resonantly forced beam-mass structures. *Nonlinear Dynamics*, 2:77–117, 1991.